molecular pharmaceutics

Brief Article

pubs.acs.org/molecularpharmaceutics

Detection of Endogenous *K-ras* mRNA in Living Cells at a Single Base Resolution by a PNA Molecular Beacon

Yossi Kam,[†] Abraham Rubinstein,[†,‡,§] Aviram Nissan,[∥] David Halle,[∥] and Eylon Yavin*[,†]

[†]Institute for Drug Research, School of Pharmacy, Faculty of Medicine, The Hebrew University of Jerusalem, P.O. Box 12065, Jerusalem 91120, Israel

[‡]The Harvey M. Krueger Family Center for Nanoscience and Nanotechnology, Faculty of Science, The Hebrew University of Jerusalem, Jerusalem 91904, Israel

[§]The David R. Bloom Center of Pharmacy, School of Pharmacy, Faculty of Medicine, The Hebrew University of Jerusalem, Jerusalem, Israel

[∥]Department of Surgery, Hadassah—Hebrew University Medical Center, Mount Scopus, P.O. Box 24035, Jerusalem 91240, Israel

Supporting Information

ABSTRACT: Detection of mRNA alterations is a promising approach for identifying biomarkers as means of differentiating benign from malignant lesions. By choosing the *KRAS* oncogene as a target gene, two types of molecular beacons (MBs) based on either phosphothioated DNA (PS-DNA-MB) or peptide nucleic acid (TO-PNA-MB, where TO = thiazole orange) were synthesized and compared *in vitro* and *in vivo*. Their specificity was examined in wild-type *KRAS* (HT29) or codon 12 point mutation (Panc-1, SW480) cells. Incubation of both beacons with total RNA extracted from the Panc-1 cell line (fully complementary sequence) showed a fluorescent signal for both beacons. Major differences were observed, however, for single mismatch mRNA transcripts in cell lines HT29 and SW480. PS-DNA-MB weakly discriminated such single mismatches in comparison to TO-PNA-MB, which was profoundly more sensitive. Cell transfection of TO-PNA-MB with the aid of PEI resulted in fluorescence in cells expressing the fully complementary RNA transcript (Panc-1) but undetectable fluorescence in cells expressing the *K-ras* mRNA that has a single mismatch to the designed TO-PNA-MB (HT29). A weaker fluorescent signal was also detected in SW480 cells; however, these cells express approximately one-fifth of the target mRNA of the designed TO-PNA-MB. In contrast, PS-DNA-MB showed no fluorescence in all cell lines tested post PEI transfection. Based on the fast hybridization kinetics and on the single mismatch discrimination found for TO-PNA-MB we believe that such molecular beacons are promising for *in vivo* real-time imaging of endogenous mRNA with single nucleotide polymorphism (SNP) resolution.

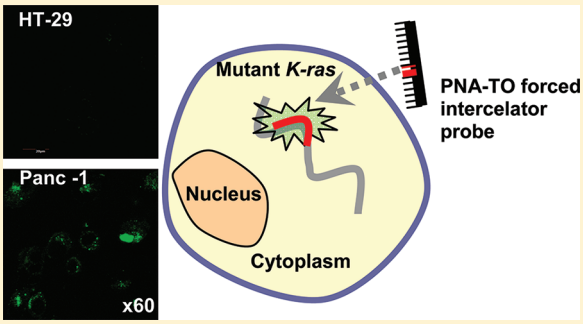

KEYWORDS: *hybridization, in vivo imaging, KRAS oncogene, molecular beacon, mRNA, peptide nucleic acids*

INTRODUCTION

Detection of mRNA alteration, either through somatic mutations or alterations in gene expression, is a promising approach for identifying cancer cells.[1,2] The ability to detect, localize, quantify and monitor such molecular alterations *in vivo* may set the bench for *in vivo* real-time imaging modality assisting in tumor diagnosis and staging.[1−3] One factor limiting molecular imaging is that most currently used probes are monochromatic and emit continuously. This dramatically reduces sensitivity even if the probe is highly specific.[4,5] In this regard, a promising approach is based on the use of molecular beacons (MBs).[6−20] These are dual-labeled oligonucleotide hairpin probes with a fluorophore at one end and a quencher at the other end. Hybridization with the target nucleic acid sequence opens the hairpin structure and spatially separates the fluorophore from quencher, allowing a fluorescence signal to be generated upon fluorophore excitation.[21]

Several studies have shown the exploitation of MBs for the detection of endogenous mRNA and microRNA[9,22−38] as well as viral mRNA in living cells.[39−42] These studies highlight the potential of such molecules to track mRNA levels and their localization in cells providing a powerful tool for diagnostics and biochemical elucidation of intracellular processes.

Peptide nucleic acids (PNAs) are oligonucleotide mimics based on an *N*-(2-aminoethyl)glycine backbone that bind to DNA or RNA via Watson−Crick base-pairing rules.[43] Due to the lack of a negatively charged backbone, hybridization of PNA occurs without electrostatic repulsion, resulting in a stronger and more rapid hybridization compared to analogous

Received: October 5, 2011
Revised: January 28, 2012
Accepted: January 30, 2012
Published: January 30, 2012

DNA:DNA or DNA:RNA duplexes. Thus, the specific site of hybridization is less sensitive to mRNA secondary and tertiary structures. Furthermore, their stability in biological medium[44] and their low toxicity make PNAs attractive for use in human diagnostic and therapeutic applications. PNA-beacons and the related "light up probes" have been described by others[45] and display the advantages of higher selectivity and simpler design.[46] PNA beacons, lacking the stem region, bearing a thiazole orange (TO) dye as a surrogate base, were shown to elicit a fluorescent signal upon binding to cDNA.[47] In a recent study by Seitz and co-workers, the capacity of such PNA based probes to detect specific viral mRNA in infected living cells was established.[48]

In this study the *KRAS* oncogene was selected as a model target, mainly because point mutations in codon 12 of the *KRAS* gene are well characterized in many cell lines and tumor types.[49] The study was undertaken with the aim of comparing two types of MB probes: phosphothioated (PS) DNA base molecular beacon (PS-DNA-MB) and thiazole orange modified peptide nucleic acid molecular beacon (TO-PNA-MB) in target accessibility and stability. TO-PNA-MB was shown to discriminate SNP in the *KRAS* gene both *in vitro* and *in vivo*. To the best of our knowledge, this is the first time that such single mismatch discrimination is shown by a MB in living cells.

EXPERIMENTAL SECTION

Materials and Instrumentation. All materials were purchased from Sigma, St. Louis, MO, USA, unless otherwise stated. All solvents were analytical grade. Water was purified by reverse osmosis. HPLC purification was performed on a Shimadzu LC-1090 system using a semipreparative C18 reverse-phase column (Phenomenex, Jupiter 300 A). Proton NMR was recorded on a 300 MHz Bruker NMR using deuterated solvents as internal standards. Mass analysis of TO-PNA-MB was acquired on a MALDI-TOF MS (Voyager De Pro, Applied Biosystems, CA, USA).

Cell Lines and Culture. PANC-1 (human pancreatic carcinoma, epithelial-like), SW-480 (human colon adenocarcinoma) and HT-29 (human colon adenocarcinoma grade II) cell lines were purchased from the American Type Culture Collection (ATCC, Manassas, VA, USA). All cells were cultured (37 °C, 5% CO_2), in DMEM medium supplemented with 10% fetal calf serum, 2 mM L-glutamine and 100 mg/mL streptomycin (Beit Haemek, Israel).

Molecular Beacons: Design and Synthesis. The sequences of the phosphothioated (PS) molecular beacon (PS-DNA-MB) and the thiazole orange peptide nucleic acid molecular beacon (TO-PNA-MB) were designed for targeting mutant *K-ras* (GAT) as expressed in Panc-1 cells (Table 1). The TO-PNA-MB sequence contained the thiazole orange (TO) dye as a surrogate base. The position of the TO along the PNA sequence was designed such that the mismatch (mutant) base is adjacent to the TO. This sequence design ensured that hybridization of the TO-PNA with mismatched targets resulted in minimal fluorescence.

Table 1. Various Codon-12 *KRAS* Targets in Cell Lines

cell line	SNP *K-ras* mutation
Panc-1[a]	GCT GAT GGC
HT-29	GCT GGT GGC
SW-480	GCT GTT GGC

[a]Targeted sequence of the MB's.

The PS-DNA-MB was designed as a hairpin where one arm of the stem and the loop region were complementary to a segment of the *KRAS* mutant target gene.[13] All PS-DNA-MB constructs as well as linear DNA probes (with Cy5 at the 5′ end) were synthesized by Integrated DNA Technologies (IDT, Coralville, IA, USA). All target sequences were 54 bases long (see sequences in Table 2).

Synthesis of PNA Monomer with TO as Surrogate Base. Fmoc-PNA-TO monomer (compound **3**, Scheme 2) and the dye TO-CH_2COOH were synthesized according to previous procedures[48,50] by using, however, a different protecting group strategy for PNA backbone synthesis (*vide post*).

1. Synthesis of TO-PNA Backbone. *Synthesis of 1-(tert-Butyloxycarbonyl)ethylenediamine.* A solution of di-*tert*-butyl dicarbonate (6.1 g, 28 mmol) in dichloromethane (400 mL) was added dropwise to a solution of ethylenediamine (11.2 mL, 166.7 mmol) in dichloromethane (50 mL) over 6 h with vigorous stirring. Stirring was continued for 24 h at room temperature. After concentration to an oily residue, the reaction mixture was dissolved in aqueous sodium carbonate (2 M, 300 mL) and extracted with dichloromethane (2 × 300 mL). The organic layer was dried (anhydrous $MgSO_4$) and the solvent evaporated under reduced pressure to yield the desired product as a colorless viscous liquid. Yield: 95%. ESI MS: m/z 161.02, calcd 160.21.

^{1}H NMR ($CDCl_3$): 4.89 (br, 1H, NH), 3.18 (dt, 2H, CH_2CH_2NH), 2.80 (t, 2H, CH_2CH_2NH), 1.60 (br, 2H, NH), 1.44 (s, 9H, tBu).

2. Synthesis of N-[(tert-Butoxycarbonyl)aminoethyl]glycine tert-Butyl Ester. 1-(*tert*-Butoxycarbonyl)aminoethylamine (16 g, 99.8 mmol) was dissolved in 200 mL of methylene chloride together with 2 equiv (34.8 mL, 199.6 mmol) of *N,N*-diisopropyethylamine (DIEA). After cooling the mixture to 0 °C, 1 equiv (14.75 mL, 99.8 mmol) of tBu-bromoacetate was added dropwise over a period of 6 h. The reaction mixture was stirred overnight. The precipitate was filtrated off, and the solvents were removed under vacuum. The resulting gum was distributed between 300 mL of H_2O and 300 mL of dichloromethane. The aqueous phase was washed with dichloromethane (4 × 200 mL). The organic fractions were pooled and dried over sodium sulfate. After the solids were filtered off, dichloromethane was evaporated to dryness. The desired product was achieved after silica gel purification (0–10% MeOH gradient in EtOAc). Yield: 73%. ESI MS: m/z 275.2, calcd 274.36.

^{1}H NMR ($CDCl_3$): 5.05 (br s, 1H, NH), 3.28 (s, 2H, CH_2CO), 3.18 (dt, 2H, CH_2CH_2NH), 2.80 (t, 2H, CH_2CH_2NH), 1.46 (s, 18H, Boc + OtBu).

3. Coupling TO-CH_2COOH to the N-[(tert-Butoxycarbonyl)aminoethyl]glycine tert-Butyl Ester Backbone. TO-CH_2COOH (176 mg, 0.5 mmol) was suspended in 2 mL of dry *N,N*-dimethylformamide (DMF) in an ice cold bath. To this suspension, 1.5 equiv (156 mg, 0.75 mmol) of *N,N′*-dicyclohexylcarbodiimide and 1.1 equiv (72.9 mg, 0.55 mmol) of *N*-hydroxybenzotriazole were added. The reaction mixture was stirred at 0 °C for 30 min. 1.5 equiv (207 mg, 0.75 mmol) of freshly prepared PNA backbone dissolved in 2 mL of DMF was added in portions. After reaching room temperature the reaction mixture was stirred for 48 h, filtered under reduced pressure and evaporated. Purification was achieved by silica gel column chromatography using an 8:2 chloroform:methanol

Table 2. The Synthetic DNA Oligomers Used in the *in Vitro* Hybridization Studies

name	description	mutation	construct[a]
WT	wild type; single mismatch to the TO binding site (as in HT-29 cells)		GTA GTT GGA GCT GGT GGC GTA GGC AAG AGT GCC TTG ACG ATA CAG CTA ATT CAG
comp-DNA	no mismatches (as in Panc-1 cells)	GGT → GAT	GTA GTT GGA GCT GAT GGC GTA GGC AAG AGT GCC TTG ACG ATA CAG CTA ATT CAG
1 mm	one adjacent mismatch to TO binding site		GTA GTT GGA GC*G* GAT GGC GTA GGC AAG AGT GCC TTG ACG ATA CAG CTA ATT CAG
2 mm	two adjacent mismatches to the TO binding site		GTA GTT GGA G*AG* GAT GGC GTA GGC AAG AGT GCC TTG ACG ATA CAG CTA ATT CAG
1 mm/1 mm	single mismatch on either side of the TO binding site		GTA GTT GGA GC*G* GGT GGC GTA GGC AAG AGT GCC TTG ACG ATA CAG CTA ATT CAG
2 mm/2 mm	two mismatches on either side of TO binding site		GTA GTT GGA G*AG* GGC GGC GTA GGC AAG AGT GCC TTG ACG ATA CAG CTA ATT CAG

[a]Underlined: complementary base to TO. Bold: site of mutation in *K-ras*. Italic: mismatch site.

mixture as eluent (compound **1**, 0.175 mmol, 35% yield). ESI MS: *m/z* 605.77, calcd 605.27.

^{1}H NMR ($CDCl_3$): 8.7 (Ar, d, 1H), 7.6 (s, 1H, Ar−*N*=CH_3), 8.22 (t, 1H, Ar−H), 7.9 (t, 1H, Ar−H), 7.7−7.9 (d, 1H, Ar−H), 7.62−7.68 (t, 1H, H−Ar), 7.4−7.58 (m, H, Ar−H), 7.0 (s, 1H, NS−C=C*H*), 4.12 (s, 2H, N−CH_2CO), 3.62 (t, 2H, NH−CH_2−CH_2−N), 3.4 (overlap, 2H, NH−CH_2−CH_2−N), 1.48 (s, 9H, C−(CH_3)$_3$), 1.28 (s, 9H, C−(CH_3)$_3$).

Simultaneous cleavage of *t*-BOC and *t*-butyl ester from compound **1** (Scheme 2) was performed using a trifluoroacetic acid:DCM 1:1 solution stirred for 3 h at room temperature. Deprotected product was precipitated from diethyl ether and immediately used for the next synthetic step (compound **2**, Scheme 2, 0.148 mmol, 85% yield). ESI MS: *m/z* 449.20, calcd 448.28.

Compound **2** (0.11 mmol) was dissolved in 2 mL of DMF with 2,6-lutidine (0.242 mmol) and stirred at room temperature for 30 min. Next, 9-fluorenylmethoxycarbonyl-succinimidyl ester (FMOC-OSu, 0.121 mmol) was added in portions, and the reaction mixture was stirred for 24 h. Solvents were removed under reduced pressure, and product was precipitated from water, filtered off and dried under vacuum. Purification was achieved by silica gel column chromatography using an 8:2 chloroform:methanol mixture as eluent (compound **3**, Scheme 2, 52 nmol, 35% yield). ESI MS: *m/z* 671.4, calcd 671.78.

^{1}H NMR (300 MHz): (DMSO-d_6): δ = 8.72 (d, 1H, Ar−H), 8.52 (d, 1H, Ar−H), 8.0 (d, 1H, Ar−H), 7.92−7.90 (m, 2H, Fmoc-H), 7.86 (m, 2H, Ar−H), 7.7 (m, 1H, Ar−H), 7.68 (m, 2H, Fmoc-H), 7.58 (m, 1H, Ar−H), 7.54 (m, 1H, Ar−H), 7.4 (m, 1H, Ar−H), 7.35 (m, 2H, Fmoc-H), 7.33 (m, 2H, Fmoc-H), 6.88 (s, 1H, cyanin-H), 4.8 (d, 2H, Fmoc-CH_2), 3.96 (s, 3H, Me-H)).

Synthesis of TO-PNA-MB. The TO-PNA-MB sequence was identical to that of the PS-DNA-MB, excluding the stem segment tail. PNA synthesis was performed using the Fmoc solid-phase synthesis on Fmoc-Lys (Boc)-Novasyn-TGA resin as previously described.[51]

Cleavage of the final PNA product from the solid support was performed in trifluoroacetic acid and *m*-cresol (95%:5%). Diethyl ether was added, and the solid precipitate was collected, dissolved in water, frozen and lyophilized. PNA was purified and analyzed by HPLC on a Phenomenex C18 column using acetonitrile and 0.1% TFA in water as eluents (for HPLC chromatogram and conditions see Figure S1 in the Supporting Information). PNA purity was verified by MALDI-TOF MS (Figure S2 in the Supporting Information). PNA was found to be >90% pure. M_{calc} = 5283.82; M_{found} = 5285.96. In our study, sample concentration was calculated by using ε_{TO} according to published values for TO situated between T and A in the designed PNA sequence[52] and by nanodrop measurement at 260 nm.

Hybridization Assays with Synthetic Constructs. PS-DNA-MB and TO-PNA-MB were tested *in vitro* for their ability to hybridize to 54 base long synthetic DNA targets (Table 2) by incubating (60 min, 37 °C) 50 nM of each MB probe with 50 nM of the target sequences in a 96-well plate. The incubation was carried out in hybridization buffer (20 mM Tris-HCl, 50 mM KCl, 10 mM $MgCl_2$, pH = 8). The fluorescence intensity of each well was measured (λ_{Ex} 495 nm; λ_{Em} 521 nm) by a microplate reader (Synergy HT Multi-Mode, Biotek, Winooski, VT, USA). Fluorescence measured from the different sequences was normalized to the fluorescence obtained from a fully complementary sequence (Comp-DNA). Hybridization rate was assessed by repeating the above incubation with Comp-DNA target (Table 2) over 90 min and recording the fluorescence intensity at 5 min intervals. In all hybridization experiments, wells without target sequences that included PS-DNA-MB or TO-PNA-MB were used as internal controls to account for intrinsic changes of fluorescence with time.

Hybridization Assay with Total RNA. PS-DNA-MB or TO-PNA-MB was incubated with 1 μg of total RNA isolated from Panc-1 cells that express the *KRAS* gene with a codon 12 GGT to GAT point mutation[53] that is fully complementary to both PS-DNA-MB and TO-PNA-MB. Total RNA was similarly isolated from HT-29 cells expressing wild-type *K-ras* that includes a unique single base mismatch to Panc-1 (GGT) and SW-480 cells expressing the *KRAS* gene with a GGT → GTT point mutation.[54]

RNA was isolated from the cells by using an RNA isolation kit (TRI reagent) according to the manufacture instructed protocol. One microgram of the extracted RNA was incubated (60 min, 50 °C) with 100 nM PS-DNA-MB or TO-PNA-MB. The resulting fluorescence was monitored in a microplate reader. The fluorescence intensity obtained upon incubation of the various types of MBs with the RNA extract isolated from the Panc-1 cells (full complementary target) was determined as 100% for each type of MB for comparing absolute fluorescence of both probes. These values were then compared to the fluorescence intensity readings obtained upon incubation of the MBs with the RNA extracts isolated from HT-29 and SW-480 cells.

Hybridization Assay in Living Cells. *Cell Preparation.* 48 h prior to hybridization, PANC-1, SW-480 and HT-29 were plated separately, on chamber slides (Ibidi GmbH, Munich, Germany) until reaching 70−80% confluence.

Cells were washed with serum free DMEM approximately 1 h before the transfection mixture was added to each well. TO-PNA-MB was hybridized for 10 min with a partly complementary Cy-5 labeled DNA oligonucleotide (1:1 ratio) at 80 °C, followed by a slow cool down to room temperature.

Living Cell Hybridization and Imaging. Transfection of the different MBs in living cells was performed using polyethylenimine (PEI) as a transfection agent. Transfection of TO-PNA-MB was achieved by annealing the partly complementary Cy5-labeled DNA that results in a DNA overhang (Scheme 1C) that was utilized to generate a stable polyplex with PEI.[55]

Scheme 1. Detection of *K-ras* mRNA Performed Using (A) TO-PNA-MB probe or (B) Classical PS-DNA-MB Probe and (C) Cell Transfection of the MBs Performed Using Polyplexes Based on Polyethylenimine (PEI)[a]

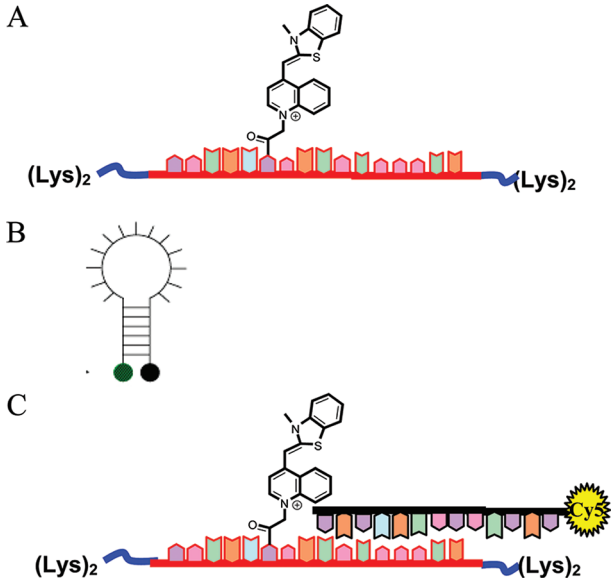

[a]In order to form a stable complex, the TO-PNA-MB probe was first hybridized to Cy5-labeled DNA that is partly complementary to the PNA sequence.

In a separate test tube, 30 μL of linear 10 μM PEI (corresponding to 5.47 mM in terms of nitrogen residues) was diluted in 20 μL of Opti-MEM medium to a final volume of 50 μL. 50 μM PNA/DNA complex was added to the PEI solution and vortexed immediately. After 15 min of incubation, polyplexes were diluted (×3.3) and 20 μL of polyplexes was added to each well. Cells were incubated (30 min, 37 °C) in a humidified atmosphere containing 5% CO_2 before medium containing 20% fetal calf serum was added to each well. 24 h later, the medium was replaced with a fresh complete medium and incubated for an additional 24 h. Cells were washed with PBS (×3) and imaged 48 h post transfection using a confocal microscope. PS-MB transfection was performed as described for TO-PNA-MB but without the need for DNA annealing. A control experiment was performed using a linear probe (Cy5-labeled DNA) to verify transfection efficacy (see probe structures in Scheme 1).

Quantification of Fluorescence in Living Cells. In living cell experiments, quantification of fluorescent was performed using ImageJ 1.40g (http://rsb.info.nih.gov/ij/). TIF images were cropped identically with the same area per analysis. ImageJ was used to measure the integrated optical density (IOD) of fluoresce intensity from a 119 × 87 pixel rectangle (region of interest, ROI) containing the same number of cells. IOD is defined as the product of optical density multiplied by the area (in pixel units). Several IODs were integrated (sum of IODs) for each cell line/MB.

Zeta Potential Measurements. To ascertain interaction of the PNA/DNA and PS-DNA-MB with polyplexes, zeta potential was measured at 25 °C using a Zetasizer Nano-Z (Malvern Instruments, Malvern, U.K.). A 20 μL aliquot of each polyplex was diluted with 980 μL of water prior to the analysis.

RESULTS

Design and Synthesis of MBs. To explore the potential of MB based probes as diagnostic tools for the early detection of cancer, two types of molecular beacons were examined for their hybridization capabilities toward various *K-ras* targets (Scheme 1). The first MB was the classic stabilized hairpin construct which consists of a phosphorothioated DNA (PS-DNA-MB) labeled with FITC as fluorophore and black hole quencher (BHQ) as quencher (Scheme 1B). The other MB was a PNA sequence containing TO as a surrogate base (TO-PNA-MB)[56](Scheme 1A). This MB was synthesized in our laboratory using standard solid phase synthesis as previously described.[51] To prepare the PNA-TO monomer (compound **3**, Scheme 2), the PNA backbone was synthesized in one simple synthetic step (Scheme 2) by

Scheme 2. Synthesis of TO-PNA Monomer[a]

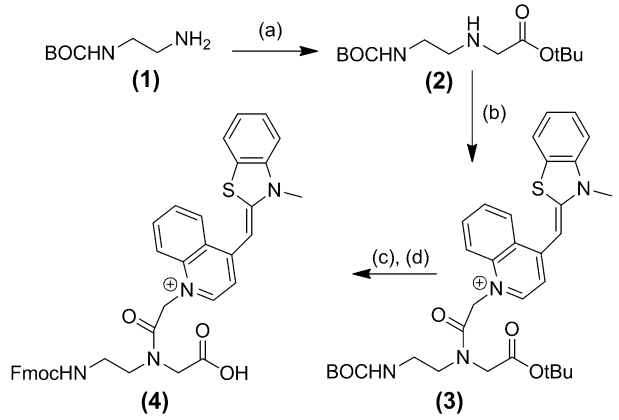

[a]Reagents and conditions: (a) tBu-bromoacetate, DIEA; (b) TO-CH_2COOH, DCC, HOBT; (c) TFA, DCM; (d) Fmoc-OSu, 2,6-lutidine.

reacting Boc-protected ethylenediamine with *t*-butyl bromoacetate, both commercially available materials. Introducing the TO surrogate base was accomplished with dicyclohexylcarbodiimide coupling followed by a TFA treatment to deprotect both BOC and tBu-ester groups. Finally, Fmoc was introduced to primary amine resulting in the desired monomer. To improve water solubility, two L-lysines were introduced at both C- and N-termini of the PNA.

The various *K-ras* targets are shown in Table 1.

Hybridization of MBs with Synthetic DNA. The various synthetic DNA targets as well as MB sequences are detailed in Table 2 and Table 3, respectively. Mismatches were added in a systematic manner on both sides of the complementary base to TO. Thus, synthetic DNA of 1 to 4 mismatches was tested with both types of MBs by monitoring fluorescence of the MBs after hybridization to the various synthetic ssDNAs.

Table 3. The Design of the PS-DNA-MB, the TO-PNA-MB, and the Linear Probe Aimed at Targeting Comp-DNA (*K-ras* Codon 12 GGT → GAT) and the DNA Sequence Used for Conjugating the PNA with PEI for Cell Transfection

name	design (5′→3′)	comment
PS-DNA-MB	FITC−CCT ACG CCA **TCA** GCT CCG TAG G-BHQ[a]	classic, hairpin, MB
TO-PNA-MB	CCT ACG CCA **T-TO-**AGCTCC	TO -containing PNA MB
DNA hybrid	Cy5-GGC GTA GGA CAC CGA[a]	the DNA/PNA construct allows PEI complexation for cell transfection
linear probe	Cy-5-CCC CTT CTC AAC CCC ACT	control

[a]The underlined bases are those added to form a stem.

The magnitude of MB *in vitro* hybridization toward synthetic DNA targets is shown in Figure 1. Generally, there was

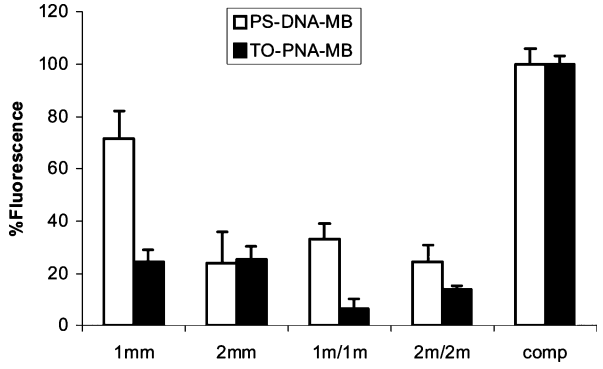

Figure 1. Specificity analysis: the effect of adjunct, single mismatch ("1mm") or 2 mismatches ("2mm") on the magnitude (expressed in % of the fluorescence of the fully complementary sequence "comp", right two columns) of the *in vitro* hybridization of *K-ras* PS-DNA-MB (empty columns) and TO-PNA-MB (filled columns) toward the synthetic targets described in Table 2 after 60 min incubation. Shown are the mean values of 4 different experiments ± SD.

comparable mismatch sensitivity for both MBs as seen for the multiple mismatch sites. When 2 or 4 adjacent mismatches (2m or 2m/2m in Figure 1) were introduced on either side of the base that was complementary to TO, both MBs gave weak and very similar fluorescent read-outs. PS-DNA-MB seems to be less sensitive to a single mismatch which is most likely related to MB design. It is expected that hybridization takes place between TO-PNA-MB and a DNA strand that has a single mismatch. Even so, as this mismatch is adjacent to the TO base surrogate, fluorescence is diminished as a consequence of TO flexibility within the local environment of the mismatch.[47,56] This behavior would be irrelevant for PS-DNA-MB.

The hybridization rates of the two MBs toward Comp-DNA (Table 2), consisting of a sequence that is fully complementary to the designed MBs (as found in Panc-1 cells), are shown in Figure 2. Figure 2A shows similar signal-to-noise ratios of ×14 and ×10 for the TO-PNA-MB and PS-DNA-MB, respectively, in the presence and absence of target DNA. Figure 2B clearly shows rapid hybridization of the TO-PNA-MB to Comp-DNA in comparison to a sluggish hybridization for PS-DNA-MB, reaching a maximal fluorescence only after ca. 190 min.

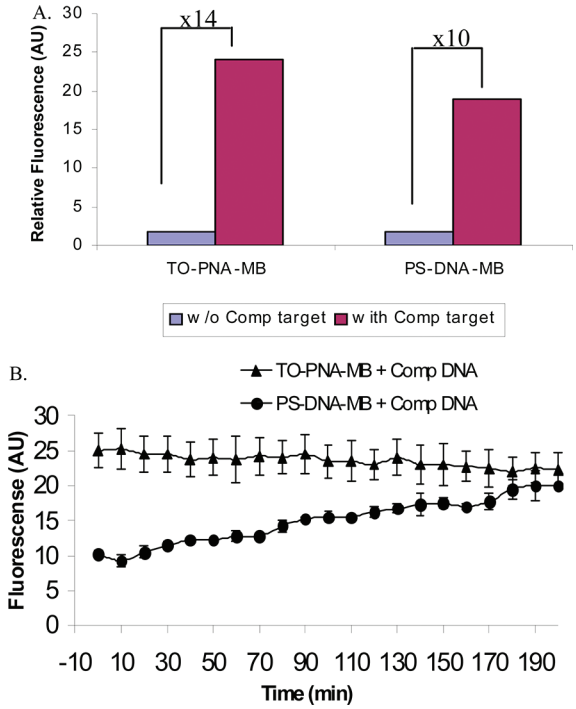

Figure 2. *In vitro* hybridization rates of PS-DNA-MB (circles) and TO-PNA-MB (triangles) with the DNA-Comp target (Table 2). Panel A shows signal-to-noise ratios for TO-PNA-MB and PS-DNA-MB in the presence and absence of target DNA. Panel B shows the hybridization kinetics of the two MBs toward Comp-DNA consisting of a sequence that is fully complementary to the designed MBs (as found in Panc-1 cells). Shown are the mean values of 3 different experiments ± SD.

Hybridization of MBs with Extracted Total RNA. The competence of the PS-DNA-MB and TO-PNA-MB to hybridize with total RNA extracts (1 μg/well) was compared. The results of the hybridization studies conducted with total RNA extracted from HT-29, Panc-1 and SW-480 cells are shown in Figure 3. The value of the fluorescence resulting from

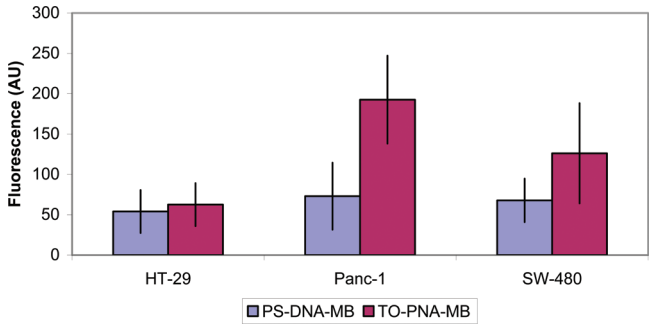

Figure 3. Hybridization (37 °C) of PS-DNAMB and TO-PNA-MB with 1 μg of total RNA extracted from HT-29, Panc-1 and SW-480 cells. Absolute fluorescence values are given (arbitrary units). Shown are the mean values of 3 different experiments ± SD. *p < 0.0001(Student's t test).

the hybridization of each MB with the Panc-1 RNA was set to 100% in order to compare the absolute fluorescent signals from both types of beacons. The fluorescence obtained upon incubation of the two MBs with the HT-29 RNA and SW-480 RNA was compared, accordingly. Figure 3 demonstrates that the most intensive fluorescence was obtained upon

dx.doi.org/10.1021/mp200505k | *Mol. Pharmaceutics* 2012, 9, 685−693

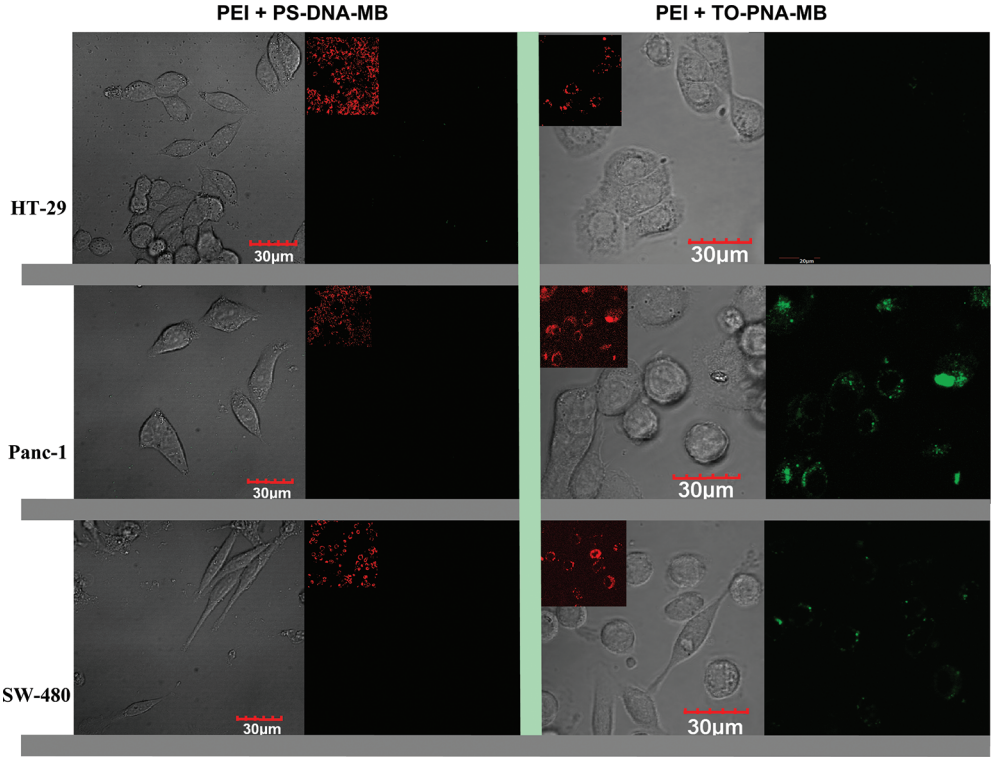

Figure 4. Confocal laser scanning microscopy images (×60) of live HT-29, Panc-1 and SW-480 cells following MB transfection (using PEI) after 48 h incubation. Control experiment to ascertain transfection employed a linear probe labeled with Cy5 (small image/right) and DNA hybrid (small image/left) of the PNA/DNA hybrid complex. Images were recorded using a 488 nm laser (TO or FITC excitation) and a 649 nm laser (for Cy5 excitation).

incubation of the TO-PNA-MB with RNA from Panc-1. The fluorescence obtained for PS-DNA-MB was about 4-fold weaker and was similar to that obtained for TO-PNA-MB with RNA from HT-29. The data generally shows that TO-PNA-MB was superior to PS-DNA-MB in discriminating cellular RNA of both HT-29 and SW-480 cells. In fact, PS-DNA-MB gave a similar and relatively weak fluorescent signal for all three extracted RNAs, highlighting the inability of this MB to discriminate single mismatches. In comparison, TO-PNA-MB showed a significant difference in fluorescence between RNA isolated from Panc-1 to that isolated from HT-29. The SW-480 RNA extract, on the other hand, gave a relatively strong fluorescent signal upon hybridization with TO-PNA-MB. This, however, can be explained by the fact that these cells indeed predominantly express a certain mutation in *K-ras* (GGT → GTT) but they also express a certain level of *K-ras* mutation (ca. 20%) that is found in Panc-1 cells (GGT → GAT).[57]

Hybridization of MBs in Live Cells. Incubating TO-PNA-MB (in complex with PEI) with cells expressing the specific mutant *K-ras* (Panc-1) resulted in relatively high fluorescence in comparison to the low fluorescence obtained in wild type *K-ras* cells (HT-29) (Figure 4). Weaker fluorescence intensity was observed in the SW-480 cells bearing a different *K-ras* mutation. In comparison, PS-DNA-MB (transfected with the aid of PEI) showed negligible fluorescence regardless of the different *K-ras* expressing cell lines. This result is in agreement with that obtained for total RNA extracted from cells (Figure 3). The absolute fluorescent signal for PS-DNA-MB, which was weak for all total RNAs examined, is manifested by the very low fluorescent signal observed for PS-PNA-MB in living cells (Figure 4). These results demonstrate the superior kinetics, target accessibility and specificity of TO-PNA-MB compared to PS-DNA-MB.

To ensure that transfection was indeed achieved for all cell lines, PEI was complexed with a linear DNA probe (labeled with Cy5) and the transfection was repeated using the same conditions (DNA concentration and ratio of DNA:PEI) as for MBs (Scheme 2C). The Cy-5 staining observed in all cells (Figure 4, inset) demonstrates effective transfection for all three cell types examined.

Cell viability was determined for all three cell lines after PEI transfection in the presence or absence of molecular beacons (Figure S3 in the Supporting Information). Some cytotoxicity was found in all transfected cells (ca. 30−45% dead cells as expected for PEI transfection[58]) that were not affected by the addition of molecular beacons).

In order to quantify the amount of fluorescence of molecular beacons in living cells, we used the ImageJ software to analyze the integrated optical density (IOD) of the fluorescence intensity in selected regions of interest (Table 4). The results

Table 4. Quantification of Fluorescence by ImageJ Software in Living Cells by TO-PNA-MB and PS-DNA-MB after PEI Transfection

	TO-PNA-MB		PS-DNA-MB	
cell line	area[a]	sum of IOD	area[a]	sum of IOD
Panc-1	5722	44,398	34	440
HT-29	3100	19,776	10	379
SW-480	3760	29,907	22	390

[a]Area: sum of pixels detected in selected region of interest (ROI, rectangle of 119 × 87 pixels).

dx.doi.org/10.1021/mp200505k | *Mol. Pharmaceutics* 2012, 9, 685−693

are consistent with those shown for total mRNA (Figure 3), namely, low fluorescence signal by PS-DNA-MB in all cells and the highest fluorescence signal in the targeted Panc-1 cell line by TO-PNA-MB.

DISCUSSION

In this study we adapted two approaches to design MB constructs for the intracellular hybridization of *KRAS* oncogene as a target gene for the *in vivo* detection of cancer cells.

Hybridization assay of TO-PNA-MB and PS-DNA-MB with synthetic constructs revealed that both PS-DNA-MB and TO-PNA-MB demonstrated specific hybridization with it specific target (Comp-DNA probe) compared to the mismatch targets (Figure 1). However, the TO-PNA-MB probe showed significant reduction in fluorescence signal even in the presence of a single mismatch compared to the PS-DNA-MB probe (22 ± 4% and 71 ± 10%, respectively).

Hybridization kinetics was additionally affected by the different structural conformation of TO-PNA-MB (linear) vs PS-DNA-MB (stem loop) configurations. In order to achieve large fluorescence enhancement using the DNA-MB, the stem−loop hairpin structure should provide an adjustable energy penalty for hairpin opening which improves probe specificity,[59] but decreased probe kinetics. As a consequence, the loop, stem lengths, and sequences are critical design parameters for such classical molecular beacons. These issues are avoided in the TO-PNA-MB design as manifested by the fast hybridization to the target sequence (Figure 2).

This matter was further manifested once we compared the performance of PS-DNA-MB to that of TO-PNA-MB in total RNA extracts. Thus, only the TO-PNA-MB was able to significantly discriminate between the wild type (HT-29, GGT) and the *K-ras* mutant (Panc-1, GGT → GAT) (*t* test, $p < 0.0001$, Figure 3). PS-DNA-MB hybridization was practically identical for all cell lines.

The fluorescence observed upon incubation of TO-PNA-MB with total mRNA from the SW-480 cell line was in agreement with a previous report indicating the expression of the mutant GAT as well as GTT in RNA extracts of the SW-480 cell line.[57] We believe that, due to the fast as well as strong hybridization capabilities of the PNA probe to DNA/RNA targets, the TO-PNA-MB was able to hybridize with the specific *K-ras* target and induce fluorescence with SW-480 mRNA even though the target sequence (as in Panc-1) was only 20% of all the transcribed *K-ras* mRNA.

Finally, we tested the detection capability of the PS-DNA-MB and TO-PNA-MB in living cells. We used the cationic polymer PEI as transfection agent due to its high transfection efficiency, stability and endosomal escape ability.[60] Since the formation of the polyplexes is predominantly based on electrostatic interactions,[61] using PNA (uncharged) and PEI (positively charged) is not sufficient for formation of polyplexes. Corey and co-workers have developed a simple and efficient method for PNA cellular uptake by hybridizing PNA with a partially complementary DNA probe.[55] For efficient transfection, cationic charge is essential for efficient binding and uptake into cells.[62] Zeta potential showed positively charged polyplexes with the PNA/DNA hybrids as well as with the PS-DNA-MB probe (above 20 mV, data not shown). Control experiments were performed using a Cy5-labeled linear DNA probe in order to assess transfection as described in Scheme 1C. Indeed, live cell confocal images showed significant fluorescence following transfection into Panc-1 using the TO-PNA-MB probe compared to the PS-DNA-MB probe (Figure 4). Weak fluorescence was also observed in the SW-480, but not in the HT-29 cells. The ability of the PNA MB to exhibit higher intracellular fluorescence compared to DNA-MB probe was recently reported.[48] In this elegant study, Kummer et al. used exogenous mRNA (influenza H1N1 mRNA infected cells) as target RNA.

Here we have found that TO-PNA-MB can detect an endogenous mRNA transcripts (i.e., *kRAS* mRNA) in living cells at a single base resolution.

A previous study has used classical MBs for the detection of mutated *kRAS* in a variety of cell lines that, similarly to our study, vary by a single base in the mRNA transcript.[13] These MBs were shown to discriminate these transcripts; however, all studies were carried out in fixed cells or frozen cancer tissues.

To the best of our knowledge there is only one more example of a molecular probe that can discriminate endogenous mRNA in living cells.[63,64] These probes are autoligating probes that were shown to discriminate at an SNP resolution an rRNA transcript in bacteria. Such probes are, however, very different from DNA or PNA beacons in the sense that a chemical reaction between two DNA molecules that bind to the target mRNA must take place in order to obtain an optical readout.

We believe that this study is of high importance as it lays the basis for using such PNA-based MBs in an *in vivo* setting. PNA-based MBs are anticipated to perform as diagnostic molecules that show a minimal false positive readout and discriminate target mRNA from nontargeted transcript at a single base resolution.

CONCLUSION

Given the growing demand for real-time *in vivo* radiation-free molecular imaging for reliable diagnosis and screening, it is important to explore new systems that could be used in clinical practice.

We have compared the performance of two such MBs, namely, classical phosphothioated (PS) MB (PS-DNA-MB) and more advanced PNA-MB based on a base surrogate design (thiazole orange). In comparison to the PS-DNA-MB, the TO-PNA-MB showed fast hybridization in solution to synthetic cDNA with the ability of discriminating complementary sequence from mismatch DNA sequences even at a single base resolution.

When examined with total RNA extracts and especially in living cells, PNA-TO-MB was found to perform better than PS-DNA-MB in both hybridization kinetics and specificity to an endogenous RNA target. Overall, this study suggests TO-PNA-MB as a promising molecule for *in vivo* detection of nucleic acids that may be generally applicable for the early detection and staging of cancer as well as a variety of genetic diseases.

ASSOCIATED CONTENT

Supporting Information

RP-HPLC chromatogram and MALDI-TOF MS of TO-PNA-MB, and MTT assay for 3 cell lines transfected with PEI and MB. This material is available free of charge via the Internet at http://pubs.acs.org.

AUTHOR INFORMATION

Corresponding Author

*The Hebrew University of Jerusalem, Faculty of Medicine, School of Pharmacy, Institute for Drug Research, P.O. Box 12065, Jerusalem 91120, Israel. Tel: 972-2-6758692. Fax: 972-2-6757076. E-mail: eylony@ekmd.huji.ac.il.

Notes

The authors declare no competing financial interest.

■ ACKNOWLEDGMENTS

The results reported here are included in the dissertation project of Y.K. in partial fulfillment of his Ph.D. degree requirements at The Hebrew University of Jerusalem. The authors thank Dr. E. Wexselblatt for synthetic assistance and Prof. O. Seitz (Department of Organic and Bioorganic Chemistry, University of Berlin) for helpful comments. The work was supported in part by Research Grant No. 38813 from the Biomedical Photonics Consortium of the Israeli Ministry of Industry and Trade.

■ REFERENCES

(1) Imyanitov, E. N.; Togo, A. V.; Hanson, K. P. Searching for cancer-associated gene polymorphisms: promises and obstacles. *Cancer Lett.* **2004**, *204*, 3−14.

(2) Shi, M. M. Enabling large-scale pharmacogenetic studies by high-throughput mutation detection and genotyping technologies. *Clin. Chem.* **2001**, *47*, 164−172.

(3) Koga, Y.; Yasunaga, M.; Moriya, Y.; Akasu, T.; Fujita, S.; Yamamoto, S.; Kozu, T.; Baba, H.; Matsumura, Y. Detection of colorectal cancer cells from feces using quantitative real-time RT-PCR for colorectal cancer diagnosis. *Cancer Sci.* **2008**, *99*, 1977−1983.

(4) Kobayashi, H.; Longmire, M. R.; Ogawa, M.; Choyke, P. L. Rational chemical design of the next generation of molecular imaging probes based on physics and biology: mixing modalities, colors and signals. *Chem. Soc. Rev.* **2011**, *40*, 4626−4648.

(5) Kobayashi, H.; Ogawa, M.; Alford, R.; Choyke, P. L.; Urano, Y. New strategies for fluorescent probe design in medical diagnostic imaging. *Chem. Rev.* **2010**, *110*, 2620−2640.

(6) Sokol, D. L.; Zhang, X. L.; Lu, P. Z.; Gewitz, A. M. Real time detection of DNA RNA hybridization in living cells. *Proc. Natl. Acad. Sci. U.S.A.* **1998**, *95*, 11538−11543.

(7) Fang, X. H.; Mi, Y. M.; Li, J. W. J.; Beck, T.; Schuster, S.; Tan, W. H. Molecular beacons - Fluorogenic probes for living cell study. *Cell Biochem. Biophys.* **2002**, *37*, 71−81.

(8) Tsourkas, A.; Behlke, M. A.; Bao, G. Hybridization of 2′-O-methyl and 2′-deoxy molecular beacons to RNA and DNA targets. *Nucleic Acids Res.* **2003**, *31*, 5168−5174.

(9) Nitin, N.; Santangelo, P. J.; Kim, G.; Nie, S. M.; Bao, G. Peptide-linked molecular beacons for efficient delivery and rapid mRNA detection in living cells. *Nucleic Acids Res.* **2004**, *3*, e58.

(10) Wang, L.; Yang, C. Y. J.; Medley, C. D.; Benner, S. A.; Tan, W. H. Locked nucleic acid molecular beacons. *J. Am. Chem. Soc.* **2005**, *127*, 15664−15665.

(11) Marti, A. A.; Jockusch, S.; Stevens, N.; Ju, J.; Turro, N. J. Fluorescent hybridization probes for sensitive and selective DNA and RNA detection. *Acc. Chem. Res.* **2007**, *40*, 402−409.

(12) Dirks, R. W.; Tanke, H. J. Advances in fluorescent tracking of nucleic acids in living cells. *Biotechniques* **2006**, *40*, 489−496.

(13) Peng, X. H.; Cao, Z. H.; Xia, J. T.; Carlson, G. W.; Lewis, M. M.; Wood, W. C.; Yang, L. Real-time detection of gene expression in cancer cells using molecular beacon imaging: new strategies for cancer research. *Cancer Res.* **2005**, *65*, 1909−1917.

(14) Yang, C. J.; Wang, L.; Wu, Y.; Kim, Y.; Medley, C. D.; Lin, H.; Tan, W. Synthesis and investigation of deoxyribonucleic acid/locked nucleic acid chimeric molecular beacons. *Nucleic Acids Res.* **2007**, *35*, 4030−4041.

(15) Haner, R.; Biner, S. M.; Langenegger, S. M.; Meng, T.; Malinovskii, V. L. A highly sensitive, excimer-controlled molecular beacon. *Angew. Chem., Int. Ed.* **2010**, *49*, 1227−1230.

(16) Bao, G.; Rhee, W. J.; Tsourkas, A. Fluorescent probes for live-cell RNA detection. *Annu. Rev. Biomed. Eng.* **2009**, *11*, 25−47.

(17) Tyagi, S. Imaging intracellular RNA distribution and dynamics in living cells. *Nat. Methods* **2009**, *6*, 331−338.

(18) Santangelo, P. J. Molecular beacons and related probes for intracellular RNA imaging. *Wiley Interdiscip. Rev.: Nanomed. Nanobiotechnol.* **2010**, *2*, 11−19.

(19) Totsingan, F.; Tedeschi, T.; Sforza, S.; Corradini, R.; Marchelli, R. Highly selective single nucleotide polymorphism recogniton by a chiral (5S) PNA beacon. *Chirality* **2009**, *21*, 245−253.

(20) Kashida, H.; Takatsu, T.; Fujii, T.; Sekiguchi, K.; Liang, X. G.; Niwa, K.; Takase, T.; Yoshida, Y.; Asanuma, H. In-stem molecular beacon containing a pseudo base pair of threoninol nucleotides for the removal of background emission. *Angew. Chem., Int. Ed.* **2009**, *48*, 7044−7047.

(21) Tyagi, S.; Kramer, F. R. Molecular beacons: probes that fluoresce upon hybridization. *Nat. Biotechnol.* **1996**, *14*, 303−308.

(22) Tsuji, A.; Koshimoto, H.; Sato, Y.; Hirano, M.; Sei-Iida, Y.; Kondo, S.; Ishibashi, K. Direct observation of specific messenger RNA in a single living cell under a fluorescence microscope. *Biophys. J.* **2000**, *78*, 3260−3274.

(23) Molenaar, C.; Marras, S. A.; Slats, J. C. M.; Truffert, J. C.; Lemaitre, M.; Raap, A. K.; Dirks, R. W.; Tanke, H. J. Linear 2 ′ O-Methyl RNA probes for the visualization of RNA in living cells. *Nucleic Acids Res.* **2001**, *29*, e89.

(24) Perlette, J.; Tan, W. H. Real-time monitoring of intracellular mRNA hybridization inside single living cells. *Anal. Chem.* **2001**, *73*, 5544−5550.

(25) Bratu, D. P.; Cha, B. J.; Mhlanga, M. M.; Kramer, F. R.; Tyagi, S. Visualizing the distribution and transport of mRNAs in living cells. *Proc. Natl. Acad. Sci. U.S.A.* **2003**, *100*, 13308−13313.

(26) Nitin, N.; Bao, G. NLS peptide conjugated molecular beacons for visualizing nuclear RNA in living cells. *Bioconjugate Chem.* **2008**, *19*, 2205−2211.

(27) Shah, R.; El-Deiry, W. S. p53-dependent activation of a molecular beacon in tumor cells following exposure to doxorubicin chemotherapy. *Cancer Biol. Ther.* **2004**, *3*, 871−875.

(28) Drake, T. J.; Medley, C. D.; Sen, A.; Rogers, R. J.; Tan, W. H. Stochasticity of manganese superoxide dismutase mRNA expression in breast carcinoma cells by molecular beacon imaging. *ChemBioChem* **2005**, *6*, 2041−2047.

(29) Mhlanga, M. M.; Tyagi, S. Using tRNA-linked molecular beacons to image cytoplasmic mRNAs in live cells. *Nat. Protoc.* **2006**, *1*, 1392−1398.

(30) Chen, A. K.; Behlke, M. A.; Tsourkas, A. Sub-cellular trafficking and functionality of 2′-O-methyl and 2′-O-methyl-phosphorothioate molecular beacons. *Nucleic Acids Res.* **2009**, *37*, e149.

(31) Rhee, W. J.; Santangelo, P. J.; Jo, H.; Bao, G. Target accessibility and signal specificity in live-cell detection of BMP-4 mRNA using molecular beacons. *Nucleic Acids Res.* **2008**, *36*, e30.

(32) Simon, B.; Sandhu, M.; Myhr, K. L. Live FISH: Imaging mRNA in living neurons. *J. Neurosci. Res.* **2010**, *88*, 55−63.

(33) Gao, Y.; Qiao, G.; Zhuo, L.; Li, N.; Liu, Y.; Tang, B. A tumor mRNA-mediated bi-photosensitizer molecular beacon as an efficient imaging and photosensitizing agent. *Chem. Commun.* **2011**, *47*, 5316−5318.

(34) Okabe, K.; Harada, Y.; Zhang, J.; Tadakuma, H.; Tani, T.; Funatsu, T. Real time monitoring of endogenous cytoplasmic mRNA using linear antisense 2 ′-O-methyl RNA probes in living cells. *Nucleic Acids Res.* **2011**, *39*, e20.

(35) Dong, H.; Ding, L.; Yan, F.; Ji, H.; Ju, H. The use of polyethylenimine-grafted graphene nanoribbon for cellular delivery of locked nucleic acid modified molecular beacon for recognition of microRNA. *Biomaterials* **2011**, *32*, 3875−3882.

(36) Kang, W. J.; Cho, Y. L.; Chae, J. R.; Lee, J. D.; Choi, K.-J.; Kim, S. Molecular beacon-based bioimaging of multiple microRNAs during myogenesis. *Biomaterials* **2011**, *32*, 1915−1922.

(37) Wang, F.; Niu, G.; Chen, X.; Cao, F. Molecular imaging of microRNAs. *Eur. J. Nucl. Med. Mol. Imaging* **2011**, *38*, 1572−1579.

(38) Qiao, G.; Gao, Y.; Li, N.; Yu, Z.; Zhuo, L.; Tang, B. Simultaneous detection of intracellular tumor mRNA with bi-color imaging based on a gold nanoparticle/molecular beacon. *Chem.—Eur. J.* **2011**, *17*, 11210−11215.

(39) Vet, J. A. M.; Majithia, A. R.; Marras, S. A. E.; Tyagi, S.; Dube, S.; Poiesz, B. J.; Kramer, F. R. Multiplex detection of four pathogenic

retroviruses using molecular beacons. *Proc. Natl. Acad. Sci. U.S.A.* **1999**, *96*, 6394−6399.
(40) Yeh, H.-Y.; Yates, M. V.; Mulchandani, A.; Chen, W. Visualizing the dynamics of viral replication in living cells via Tat peptide delivery of nuclease-resistant molecular beacons. *Proc. Natl. Acad. Sci. U.S.A.* **2008**, *105*, 17522−17525.
(41) Yeh, H.-Y.; Yates, M. V.; Mulchandania, A.; Chen, W. Molecular beacon-quantum dot-Au nanoparticle hybrid nanoprobes for visualizing virus replication in living cells. *Chem. Commun.* **2010**, *46*, 3914−3916.
(42) Cui, Z. Q.; Zhang, Z. P.; Zhang, X. E.; Wen, J. K.; Zhou, Y. F.; Xie, W. H. Visualizing the dynamic behavior of poliovirus plus-strand RNA in living host cells. *Nucleic Acids Res.* **2005**, *33*, 3245−3252.
(43) Egholm, M.; Buchardt, O.; Christensen, L.; Behrens, C.; Freier, S. M.; Driver, D. A.; Berg, R. H.; Kim, S. K.; Norden, B.; Nielsen, P. E. PNA hybridizes to complementary oligonucleotides obeying the Watson-Crick hydrogen-bonding rules. *Nature* **1993**, *365*, 566−568.
(44) Demidov, V. V.; Potaman, V. N.; Frank-Kamenetskii, M. D.; Egholm, M.; Buchard, O.; Sonnichsen, S. H.; Nielsen, P. E. Stability of peptide nucleic acids in human serum and cellular extracts. *Biochem. Pharmacol.* **1994**, *48*, 1310−1313.
(45) Ortiz, E.; Estrada, G.; Lizardi, P. M. PNA molecular beacons for rapid detection of PCR amplicons. *Mol. Cell. Probes* **1998**, *12*, 219−226.
(46) Svanvik, N.; Nygren, J.; Westman, G.; Kubista, M. Free-probe fluorescence of light-up probes. *J. Am. Chem. Soc.* **2001**, *123*, 803−809.
(47) Bethge, L.; Jarikote, D. V.; Seitz, O. New cyanine dyes as base surrogates in PNA: Forced intercalation probes (FIT-probes) for homogeneous SNP detection. *Bioorg. Med. Chem.* **2008**, *16*, 114−125.
(48) Kummer, S.; Knoll, A.; Socher, E.; Bethge, L.; Herrmann, A.; Seitz, O. Fluorescence imaging of influenza H1N1 mRNA in living infected cells using single-chromophore FIT-PNA. *Angew. Chem., Int. Ed.* **2011**, *50*, 1931−1934.
(49) Minamoto, T.; Mai, M.; Ronai, Z. K-ras mutation: early detection in molecular diagnosis and risk assessment of colorectal, pancreas, and lung cancers- a review. *Cancer Detect. Prev.* **2000**, *24*, 1−12.
(50) Jarikote, D. V.; Kohler, O.; Socher, E.; Seitz, O. Divergent and linear solid-phase synthesis of PNA containing thiazole orange as artificial base. *Eur. J. Org. Chem.* **2005**, *15*, 3187−3195.
(51) Nielsen, P. E. PNA technology. *Methods Mol. Biol.* **2002**, *208*, 3−26.
(52) Jarikote, D. V.; Krebs, N.; Tannert, S.; Roder, B.; Seitz, O. Exploring base-pair-specific optical properties of the DNA stain thiazole orange. *Chem.—Eur. J.* **2007**, *13*, 300−310.
(53) Berrozpe, G.; Schaeffer, J.; Peinado, M. A.; Real, F. X.; Perucho, M. Comparative analysis of mutations in the p53 and K-ras genes in pancreatic cancer. *Int. J. Cancer* **1994**, *58*, 185−191.
(54) Brink, M.; de Goeij, A. F.; Weijenberg, M. P.; Roemen, G. M.; Lentjes, M. H.; Pachen, M. M.; Smits, K. M.; de Bruine, A. P.; Goldbohm, R. A.; van den Brandt, P. A. K-ras oncogene mutations in sporadic colorectal cancer in the Netherlands cohort study. *Carcinogenesis* **2003**, *24*, 703−710.
(55) Doyle, D. F.; Braasch, D. A.; Simmons, C. G.; Janowski, B. A.; Corey, D. R. Inhibition of gene expression inside cells by peptide nucleic acids: effect of mRNA target sequence, mismatched bases, and PNA length. *Biochemistry* **2001**, *40*, 53−64.
(56) Kohler, O.; Jarikote, D. V.; Seitz, O. Forced intercalation probes (FIT Probes): Thiazole orange as a fluorescent base in peptide nucleic acids for homogeneous single-nucleotide-polymorphism detection. *ChemBioChem* **2005**, *6*, 69−77.
(57) Amicarelli, G.; Adlerstein, D.; Shehi, E.; Wang, F.; Makrigiorgos, G. M. Genotype-specific signal generation based on digestion of 3-way DNA junctions: application to KRAS variation detection. *Clin. Chem.* **2006**, *52*, 1855−1863.
(58) Magadala, P.; Amiji, M. Epidermal growth factor receptor-targeted gelatin-based engineered nanocarriers for DNA delivery and transfection in human pancreatic cancer cells. *AAPS J.* **2008**, *10*, 565−576.
(59) Bonnet, G.; Tyagi, S.; Libchaber, A.; Kramer, F. R. Thermodynamic basis of the enhanced specificity of structured DNA probes. *Proc. Natl. Acad. Sci. U.S.A.* **1999**, *96*, 6171−6176.
(60) Tros de Ilarduya, C.; Sun, Y.; Duzgunes, N. Gene delivery by lipoplexes and polyplexes. *Eur. J. Pharm. Sci.* **2010**, *40*, 159−170.
(61) Tang, M. X.; Szoka, F. C. The influence of polymer structure on the interactions of cationic polymers with DNA and morphology of the resulting complexes. *Gene Ther.* **1997**, *4*, 823−832.
(62) Behr, J. P.; Demeneix, B.; Loeffler, J. P.; Perez-Mutul, J. Efficient gene transfer into mammalian primary endocrine cells with lipopolyamine-coated DNA. *Proc. Natl. Acad. Sci. U.S.A.* **1989**, *86*, 6982−6986.
(63) Sando, S.; Abe, H.; Kool, E. T. Quenched auto-ligating DNAs: multicolor identification of nucleic acids at single nucleotide resolution. *J. Am. Chem. Soc.* **2004**, *126*, 1081−1087.
(64) Franzini, R. M.; Kool, E. T. Improved templated fluorogenic probes enhance the analysis of closely related pathogenic bacteria by microscopy and flow cytometry. *Bioconjugate Chem.* **2011**, *22*, 1869−1877.